Computers, Materials & Continua
DOI:10.32604/cmc.2020.012322
Article

Tech Science Press

Mixed Convection of Non-Newtonian Erying Powell Fluid with Temperature-Dependent Viscosity over a Vertically Stretched Surface

Ahlam Aljabali[1], Abdul Rahman Mohd Kasim[1,*], Nur Syamilah Arifin[2] and Sharena Mohamad Isa[3]

[1]Centre for Mathematical Sciences, UMP, Gambang, 26300, Malaysia
[2]Faculty Computer and Mathematical Sciences, UiTM Johor, Pasir Gudang Campus, Masai, 81750, Malaysia
[3]Manufacturing Engineering Technology Section, UniKL, Italy Design Institute, Kuala Lumpur, 56100, Malaysia
[*]Corresponding Author: Abdul Rahman Mohd Kasim. Email: rahmanmohd@ump.edu.my
Received: 25 June 2020; Accepted: 21 August 2020

Abstract: The viscosity of a substance or material is intensely influenced by the temperature, especially in the field of lubricant engineering where the changeable temperature is well executed. In this paper, the problem of temperature-dependent viscosity on mixed convection flow of Eyring Powell fluid was studied together with Newtonian heating thermal boundary condition. The flow was assumed to move over a vertical stretching sheet. The model of the problem, which is in partial differential equations, was first transformed to ordinary differential equations using appropriate transformations. This approach was considered to reduce the complexity of the equations. Then, the transformed equations were solved using the Keller box method under the finite difference scheme approach. The validation process of the results was performed, and it was found to be in an excellent agreement. The results on the present computation are shown in tabular form and also graphical illustration. The major finding was observed where the skin friction and Nusselt number were boosted in the strong viscosity.

Keywords: Temperature-dependent viscosity; Erying Powell fluid; numerical solution; combined convection

1 Introduction

Advancements in the study of fluid mechanics have contributed to the significant innovation in engineering devices where it is widely used in the technological and industrial fields. The process in manufacturing these devices involves the heat transfers procedure. Heat transfers also can be found in the boundary layer flow, heat exchangers, and solar core receivers, which are visible to wind currents, fan-cooling, the manufacturing of electronic devices, cooling nuclear reactors during an emergency shutdown, low-velocity heat exchangers and electrical equipment [1–4]. Currently, this research area is emerging and has begun to gain a high interest among researchers due to the considerable applications in the engineering production comprising polymer processing. The advancement in fluid mechanics as well as heat transfer, for example, has continuously been the critical subjects in stipulating the pieces of machinery of manufactured polymers. Polymer properties, on account of their complex configuration, are different compared to viscous fluids like water or oil due to their excessive viscosity and viscoelasticity and that they are commonly non-Newtonian in nature. Some vigorous features of polymers are its retardation and relaxation criterion. In many circumstances, operations involving polymers by most manufacturing processes are generally in the laminar form as a result of their high viscosity level [5]. The action of natural buoyancy forces on the fluid flow is termed as free or natural convection. Predominantly, the natural buoyancy forces increase density gradients in the fluid that is induced by [6] and differences in the temperature. Therefore, previous literature has worked on different areas of this respective flow in varying their characteristics, such as geometries, boundary conditions, and fluid-based forms. Such flow patterns exist concurrently in both the external forcing system and internal volumetric forces that are significant either with the influence of the buoyancy forces in forced convection or with the influence of forced flow in free convection. Forced convection occurs when $\lambda \to 0$ while free convection happens when $\lambda \to \infty$. Meanwhile, if the free convection and forced convection flows act together, mixed convection flow will occur. This mixed convection happens due to the difference between surface temperature and the surrounding fluid that results in the power of buoyancy forces. Several studies have mentioned the mixed convection flow for various physical and geometrical aspects [7–12]. For example, Umavathi et al. [13] investigated the flow under free convection by considering the combined effects of variable viscosity and thermal conductivity over a vertical channel. An effect of the temperature-dependent fluid properties on the fluid-structure and heat transfer is essential in cases of moderate temperature difference cases. Studies on viscous dissipation on a vertically stretched surface for unsteady mixed convection and heat transfer have been performed by [14–18]. In [19], the unsteady natural convection in the differentially heated square cavity of a fluid of temperature-dependent viscosity has been numerically analysed. It has been noticed that thermal convection is more intensive at near the hot wall for a variable viscosity fluid, and the heat input from the hot vertical wall to the cavity exceeds the heat output to the cold vertical wall during the transient phase. An enhanced viscosity correlation has been given by [20]. Mass transfer effects on the flow through an accelerated vertical plate, as well as the combined effect of high viscosity and thermal conductivity have been studied by [21] and [22]. In [23], the unsteady natural convection was examined with temperature-dependent viscosity within a square porous cavity. In [24], a mathematical analysis of a continuous, incompressible flow of a temperature-dependent on nanofluid from a vertical stretching surface under the external magnetic field and gravitational body force effects has been carried out using the Reynolds exponential viscosity model. The examination of convective flow and heat transport of fluids with temperature-dependent properties is of a great significance for the functional value of modern fluid systems, as mentioned in [25] and [26]. Another analysis of the flow problem associated with this particular effect on temperature-dependent viscosity moving over a vertical plate has drawn some researchers' attention [27–29].

Commonly, in industries, the non-Newtonian fluid is widely used, such as Erying Powell, Power law, Maxwell and micropolar fluid models. The model considered is complex and has a preference for other fluid types. The derivation of the Power-Law model is based on the kinetic theory of liquid rather than the empirical relation, which condenses the high and low shear levels according to properties of Newtonian significance. Previously, Erying Powell fluids' flow has been numerically analysed by [30], which showed that the effects on Erying Powell to the magnetic field over a stretching area. The velocity profile declined as magnetic flux and Erying Powell fluid parameters rise in pressure. They noticed that for high Prandtl number values, the boundary layer would decrease. They also examined the increasing velocity profile by optimising suction parameter values. It displayed that the temperature of fluid decreases for a larger suction parameter. Apart from that, Ara et al. [31] focused on an investigation under exponential representation of the Erying Powell fluid flow over a shrinking surface. They investigated the increase in mass suction that improved the velocity profile, while the temperature profile displayed contrary behaviour. Besides, the thickness of the boundary layer decreased with increasing values of Prandtl number. Moreover, Malik et al.

[32] studied the movement of Erying Powel fluid over an expanding cylinder and finally found two versions namely Reynaldo's and Vogel's. They found that the boundary layer decreased for high Prandtl number values. They also examined the increase in velocity profile that depended on the suction parameter. For large values of suction parameter, the temperature profile decreased. The nature of mass and heat transfer on free and forced convection flow in a stretching cone has been observed by [33]. They noted that the flow parameters' tangential velocity varies in behaviour. Furthermore, the coefficient of skin friction increased due to the growth in the ratio of buoyancy forces. In [34], the relation of Erying Powell fluid series and numerical flow solutions with Newtonian heating has been reported. Meanwhile, the MHD flow of hyperbolic tangent fluid through a stretching cylinder and Keller box system has been studied by [35]. In addition, the Erying Powell fluid's model, has been examined under various physical conditions in [36–39].

According to most industrial and engineering applications, the flow produced by a stretching surface generates keen interest. The analysis showed that the incompressible boundary layer of mixed convection flow over a stretching surface in two dimensions could be considered as a heating environment with the Newtonian heating boundary condition. The present study explores the solution on mixed convective of Eyring Powell fluid's flow combined with temperature-dependent viscosity and embedded with thermal Newtonian heating past a vertical stretching surface. The numerical computation was performed by using the Keller box approach, and the solutions are presented through graphs and tables.

2 Problem Formulation

Consider the problem of two-dimensional incompressible Eyring Powell fluid under the mechanism of temperature-dependent viscosity embedded with thermal boundary condition known as Newtonian Heating (NH). The flow occurs over a vertical stretching sheet where it stretches in a direction and moves with uniform velocity. The *x*-axis is defined as an upward direction alongside the sheet, while *y*-axis assumes its upright direction to the surface. The basic theory on the derivation of the Eyring Powell model is constructed on the rate processes theory, which demonstrates the sheer of non-Newtonian flow.

The constitutive equation of Cauchy stress of Eyring Powell Fluid is defined as

$$\mathrm{T} = \left(\mu + \frac{1}{\tilde{\beta}\gamma}\sin^{-1}\left(\frac{1}{C^*}\gamma\right)\right)\mathrm{A}_1, \tag{1}$$

where

$$\gamma = \left(\frac{1}{2}tr(\mathrm{A}_1)^2\right)^{1/2}. \tag{2}$$

Apart from that, the second-order approximation of the $\sinh^{-1}$ function is defined as

$$\sinh^{-1}\left(\frac{1}{C^*}\gamma\right) \cong \left(\frac{\gamma}{C^*} - \frac{\gamma^3}{6C^*}\right). \tag{3}$$

In the Cartesian coordinate system, the governing equations representing Eyring Powell fluid with temperature-dependent viscosity can be expressed as

Continuity equation

$$\frac{\partial u}{\partial x} + \frac{\partial v}{\partial y} = 0 \tag{4}$$

x−**momentum equation**

$$u\frac{\partial u}{\partial x}+v\frac{\partial u}{\partial y}=-\frac{1}{\rho}\frac{\partial P}{\partial x}+\left(v+\frac{1}{\rho\tilde{\beta}C^{*}}\right)\left(\frac{\partial^2 u}{\partial x^2}+\frac{\partial^2 u}{\partial y^2}\right)-\frac{1}{3\rho\tilde{\beta}C^{*3}}\frac{\partial}{\partial x}\left(2\left(\frac{\partial u}{\partial x}\right)^2+\left(\frac{\partial u}{\partial y}+\frac{\partial v}{\partial x}\right)^2+2\left(\frac{\partial v}{\partial y}\right)^2\right)$$
$$\frac{\partial u}{\partial x}-\frac{1}{6\rho\tilde{\beta}C^{*3}}\frac{\partial}{\partial y}\left(2\left(\frac{\partial u}{\partial x}\right)^2+\left(\frac{\partial u}{\partial y}+\frac{\partial v}{\partial x}\right)^2+2\left(\frac{\partial v}{\partial y}\right)^2\right)\left(\frac{\partial u}{\partial y}+\frac{\partial v}{\partial x}\right)+\frac{1}{\rho}F_x, \tag{5}$$

y−**momentum equation**

$$u\frac{\partial v}{\partial x}+v\frac{\partial v}{\partial y}=-\frac{1}{\rho}\frac{\partial P}{\partial y}+\left(\mu+\frac{1}{\tilde{\beta}C^{*}}\right)\left(\frac{\partial^2 v}{\partial x^2}+\frac{\partial^2 v}{\partial y^2}\right)-\frac{1}{3\rho\tilde{\beta}C^{*3}}\frac{\partial}{\partial y}\left(2\left(\frac{\partial u}{\partial x}\right)^2+\left(\frac{\partial u}{\partial y}+\frac{\partial v}{\partial x}\right)^2+2\left(\frac{\partial v}{\partial y}\right)^2\right)$$
$$\frac{\partial v}{\partial y}-\frac{1}{6\rho\tilde{\beta}C^{*3}}\frac{\partial}{\partial x}\left(2\left(\frac{\partial u}{\partial x}\right)^2+\left(\frac{\partial u}{\partial y}+\frac{\partial v}{\partial x}\right)^2+2\left(\frac{\partial v}{\partial y}\right)^2\right)\left(\frac{\partial u}{\partial y}+\frac{\partial v}{\partial x}\right)+\frac{1}{\rho}F_y. \tag{6}$$

Eqs. (5) and (6) were once investigated by [40] without considering buoyancy and temperature-dependent viscosity. The complexity of momentum equations was reduced by utilizing the boundary layer theory pioneered by Prandtl (1904). Through this theory, the complicated Navier–Stokes equation can be simplified into a set of equations known as the boundary layer equations [41]. According to the principle under boundary layer theory, the velocity and temperature differential are more significant than those in the direction at right angles to the ground. Under the explanation on this simplification, the procedure is made available in which Eqs. (5) and (6) take the form

$$u\frac{\partial u}{\partial x}+v\frac{\partial u}{\partial y}=-\frac{1}{\rho}\frac{\partial P}{\partial x}+\left(v+\frac{1}{\rho\tilde{\beta}C^{*}}\right)\frac{\partial^2 u}{\partial y^2}-\frac{1}{2\rho\tilde{\beta}C^{*}}\left(\frac{\partial u}{\partial y}\right)^2\frac{\partial^2 u}{\partial y^2}+\frac{1}{\rho}F_x, \tag{7}$$

$$\frac{\partial P}{\partial y}=0. \tag{8}$$

Eq. (8) indicates that the equation is unconditional to y. If the lateral velocity is zero, then the pressure is constant. The power of volume is the forces acting on fluid flow. It is also known as the long-range arm. In general, the frequency of this force varies very slowly and works equally on all areas of fluid flow. Example of this type of forces is gravitational, given by

$$F=\rho g, \tag{9}$$

where g is the centre of gravity. In two-dimensional flows, the gravitational forces are defined as,

$$F=(F_x,F_y,0)=\rho(-g_x,-g_x,0). \tag{10}$$

The pressure, P, in the momentum equation, is the combination of hydrostatic pressure, P_h while dynamic pressure in the quiescent ambient medium, P_d. Since g is moving downwards and x-direction is upwards, the pressure gradient as described in [42] can be written as

$$-\frac{\partial p}{\partial x}=-\frac{\partial p_d}{\partial x}+\rho_\infty g_c. \tag{11}$$

Substituting Eq. (11) into Eq. (7) produces

$$u\frac{\partial u}{\partial x}+v\frac{\partial u}{\partial y}=\frac{1}{\rho}\frac{\partial}{\partial y}\left(\mu\frac{\partial u}{\partial y}\right)+\frac{1}{\rho\tilde{\beta}c}\left(\frac{\partial^2 u}{\partial y^2}\right)-\frac{1}{2\rho\tilde{\beta}c^3}\left(\frac{\partial u}{\partial y}\right)^2\frac{\partial^2 u}{\partial y^2}+\frac{1}{\rho}g(\rho_\infty-\rho). \tag{12}$$

When performing Boussinesq approximation, all consequences of variable properties are ignored except for density in the momentum equation. This approximation is used as a pure temperature effect to estimate the difference in density, which causes the flow as a result of an interaction between gravitational body force and hydrostatic pressure gradient. The maximum value is believed to be minimal, and the subsequent Taylor expansion becomes

$$\frac{\rho_\infty}{\rho}=1+\tilde{\beta}(T-T_\infty)+O(T-T_\infty). \tag{13}$$

Manipulating the Eq. (13), yields

$$\frac{\rho_\infty-\rho}{\rho}=\beta(T-T_\infty). \tag{14}$$

Therefore, after substituting Eq. (14) into Eq. (12), the continuity and energy equations are given correspondingly, which takes the form as describe in [43]

$$\frac{\partial u}{\partial x}+\frac{\partial v}{\partial y}=0 \tag{15}$$

$$u\frac{\partial u}{\partial x}+v\frac{\partial u}{\partial y}=\frac{1}{\rho}\frac{\partial}{\partial y}\left(\mu\frac{\partial u}{\partial y}\right)+\frac{1}{\rho\tilde{\beta}c}\left(\frac{\partial^2 u}{\partial y^2}\right)-\frac{1}{2\rho\tilde{\beta}c^3}\left(\frac{\partial u}{\partial y}\right)^2\frac{\partial^2 u}{\partial y^2}+\beta g(T-T_\infty), \tag{16}$$

$$\rho c_p\left(u\frac{\partial T}{\partial x}+v\frac{\partial T}{\partial y}\right)=k\left(\frac{\partial^2 T}{\partial y^2}\right). \tag{17}$$

The present flow analysis is subjected to the following boundary conditions

$$\begin{aligned}&u=u_w(x)=ax,\ v=0,\ \frac{\partial T}{\partial y}=-h_sT(\text{NH})\text{ at }y=0,\\&u\to 0,\ T\to T_\infty\text{ as }y\to\infty,\end{aligned} \tag{18}$$

where $u_w(x)$ is taken as velocity of the stretched surface with a a as positive constant, (u,v), v, T, T_∞, ρ, c_p, μ, h_s, P, α, $\tilde{\beta}$ and c^* are the velocity components in x-, y-directions, kinematic viscosity, temperature, ambient temperature, density, specific heat at constant pressure, viscosity coefficient, the heat transfer parameter, a pressure, thermal diffusivity and fluid factors of the Powell' model, respectively. Meanwhile, $\tilde{\beta}$ and c^* have the dimension of $(time^{-1})$.

To obtain the set f similarity equation in the form of an ordinary differential equation, the similarity transformation variables as in Eq. (19) are adopted and applied to the Eqs. (15) to (17), which yields

$$u=axf'(\eta),\quad v=-\left(av_f\right)^{1/2}f(\eta),\quad \eta=\left(\frac{a}{v_f}\right)^{1/2}y,\quad \theta(\eta)=\frac{T-T_\infty}{T_\infty}. \tag{19}$$

To feign the temperature-dependent viscosity variable, the Reynolds exponential viscosity model is taken into account, which gives a detailed approach to

$$\mu(\theta) = \mu_0 e^{-(\beta_1\theta)} = \mu_0\left[1 - (\beta_1\theta) + O\left({\beta_1}^2\right)\right], \tag{20}$$

where fluid viscosity is assumed to vary as a linear inverse temperature function

$$\frac{1}{\mu} = \frac{1}{\mu_\infty}[1 + \gamma(T - T_\infty)],\ \text{or}\ \frac{1}{\mu} = a(T - T_r). \tag{21}$$

The resulting equations are obtained as follows

$$(1 - \alpha\theta(\eta))f'''(\eta) + Mf'''(\eta) - (f'(\eta))^2 + f(\eta)f''(\eta) - BM(f''(\eta))^2 f'''(\eta) - \alpha f''(\eta)\theta'(\eta) + \lambda\theta = 0, \tag{22}$$

$$\frac{1}{\Pr}\theta''(\eta) + f(\eta)\theta'(\eta) = 0, \tag{23}$$

together with the transformed boundary conditions as

$$\begin{aligned} &f(0) = 0, \quad f'(0) = 1, \quad \theta'(0) = -\gamma(1 + \theta(0))(\text{NH}), \quad \text{at}\ \eta = 0 \\ &f'(\eta) \to 0, \quad \theta(\eta) \to 0 \quad \text{as}\ \eta \to \infty. \end{aligned} \tag{24}$$

3 Computation Procedures

The obtained solvable equations are resolved using Keller box technique in the form of established ordinary differential equations. Eqs. (22) and (23) according to boundary conditions (24) are condensed to a system of the first order. For that matter, the independent variables are demonstrated as

$$f' = u,\ u' = v,\ \text{s} = \theta,\ \theta' = s' = t. \tag{25}$$

Then the respective equations can be written as

$$(1 - \alpha\theta)v' + Mv' - u^2 + fv - BMv^2v' - \alpha vt + \lambda\theta = 0, \tag{26}$$

$$\frac{1}{\Pr}t' + ft = 0. \tag{27}$$

In Eqs. (19), (22) to (24), the notation prime ($'$) corresponds to the derivative with respect to η. Additionally, where the fluid parameters, M and B, Prandtl number, Pr, conjugate parameter, γ, viscosity parameter, α, fluid kinematic viscosity, v_f and mixed convection, λ, are defined as,

$$\begin{aligned} &M = \frac{1}{\mu_0\tilde{\beta}c}, \quad B = \frac{a^3x^2}{2c^2v_f}, \quad \Pr = \frac{\mu c_p}{k}, \quad \gamma = -\frac{h_f}{k}\left(\frac{\upsilon}{a}\right)^{1/2} \\ &\alpha = \frac{k}{\rho c_p}, \quad v_f = \mu_0/\rho, \quad \lambda = \frac{g_c\beta_T\left(T_f - T_\infty\right)}{a^2x}. \end{aligned} \tag{28}$$

The steps of Keller box techniques are as follows

i) The Eqs. (22) and (23) are reduced to a first-order arrangement.
ii) The attained system in (i) is changed to a system of algebraic equations by means of the central difference formula.
iii) The resultant in (ii) is linearized using Newton's method and prepared in matrix-vector system.
iv) The output (iii) is determined using the block-tridiagonal elimination method.

In this present mathematical model, the magnitudes of the skin friction coefficient and the Nusselt number are as follows

$$C_f \mathrm{Re}_x^{1/2} = \left(((1-\alpha\theta(0)) + M)f''(0) - \frac{B}{3}Mf''^3(0)\right);\ Nu_x \mathrm{Re}_x^{-1/2} = \gamma\left(1 + \frac{1}{\theta(0)}\right). \tag{29}$$

4 Validation Procedure

The present model is computed using the Keller box approach. The upshot of fluid parameters (M and B) representing Eyring model, Prandtl number (Pr), mixed convection parameter (λ), conjugate parameter (γ) and viscosity parameter (α) on velocity and temperature profile against η are figured via MATLAB software. The proposed method is undeniably suitable since it is proven to be unconditionally stable, even for a higher-order model. It is worth mentioning here that, the comparison between the present results with the previous existing solution for limiting case is essential to claim that the current model and its output are acceptable.

The direct comparative studies with the existing literature have been conducted to corroborate the numerical solutions acquired in this study. The Tab. 1 shows the summary of the work done by [24]. The momentum equation on particular works can be reduced to its limiting case by fixing the $B_r = 0$ and $M = 0$.

Table 1: Model by [24]

Equation involved	Boundary condition
$(1-(\alpha\theta))f''' - \alpha\theta' f'' - (f')^2 + ff'' - M^2 f' + G_r\theta + B_r\phi = 0$ $\frac{1}{\mathrm{Pr}}\theta'' + f\theta' + N_b\theta'\xi' + N_t(\theta')^2 = 0$ $\phi'' + Scf\phi' + \frac{N_t}{N_b}\theta'' = 0$	$f(0) = 0, f'(0) = 1, \theta(0) = 1,$ $\phi(0) = 1, f'(\infty) = 0,$ $\theta(\infty) = 0, \phi(\infty) = 0.$

The output from the comparative study on momentum equation shows a firm agreement, indicating that the current model and its findings are acceptable. A clear picture of this working is presented in Tab. 2. Besides, the present works also presents a comparative study on the value of $\theta(0)$ and $-\theta'(0)$ and the results were undeniably in agreement with the reports by [44] and [45]. The results on this particular matter are presented in Tab. 3.

Table 2: Comparison of value $(1-\alpha\theta(0))f''(0)$ at $\lambda = 1, B = M = 0$

α	[24]	Present
0.0	0.61617	0.615004
0.1	0.58613	0.586746
0.2	0.55398	0.550962

5 Results and Discussion

The numerical solutions obtained were analysed after undergoing proper validation process. The results were computed under the NH boundary condition for various parameters Pr, α, M, B, γ and λ. The computation was done by assigning a set of fixed values of the parameter followed by the calculation on the value of $C_f \mathrm{Re}_x^{1/2}$ and $Nu_x \mathrm{Re}_x^{-1/2}$.

Table 3: Comparison on value $\theta(0)$ and $-\theta'(0)$ at $B = \lambda = 0, M = \gamma = 1$

Pr	$\theta(0)$			$-\theta'(0)$		
	[44]	[45]	Present	[44]	[45]	Present
3	6.02577	6.05168	6.0265562	7.02577	7.05168	7.0265562
5	1.76594	1.76030	1.7657583	2.76594	2.76039	2.7657583
7	1.13510	1.11682	1.1264703	2.13511	2.11682	2.1264703
10	0.76530	0.76450	0.7610023	1.76531	1.76452	1.7610023
100	0.16110	0.14780	0.1649870	1.16115	1.14780	1.1649870

Tab. 4 depicts the variations of $C_f \mathrm{Re}_x^{1/2}$ and $Nu_x \mathrm{Re}_x^{-1/2}$ with variation of value of pertinent parameters involved. For the entire computation, the value of γ was set as 1. It was noticed that a more substantial value of Pr, λ, γ, α, M and B boosted the $Nu_x \mathrm{Re}_x^{-1/2}$. This was due to the presence on those parameters that made the convective process in the fluid flow become more active. The $C_f \mathrm{Re}_x^{1/2}$ was increased in the higher values of γ and α but showed a reduction trend in the larger values of Pr, λ, M and B. The increasing trend happened due to the strengthen on drag forces, which increased the viscosity of the fluid. Meanwhile, the lessening was due to the weakness in the resistance of fluid with the surface.

Table 4: Numerical results of $C_f \mathrm{Re}_x^{1/2}$, $Nu_x \mathrm{Re}_x^{-1/2}$ and various values of Pr, α, M, B, λ and γ

Pr	α	M	B	γ	λ	$\theta(0)$	$C_f \mathrm{Re}_x{}^{1/2}$	$Nu_x \mathrm{Re}_x{}^{-1/2}$
7	0.1	1	0.1	1	0.1	0.381319	−1.387882	0.618680
9						0.331691	−1.391323	0.668308
12						0.252203	−1.394975	0.747796
10	0. 15					0.317005	−1.389797	0.682994
	0.3					0.303985	−1.382803	0.696014
	0.4					0.292714	−1.378598	0.707285
10	0.1	0.5				0.322521	−1.073225	0.677478
		0.9				0.315830	−1.226956	0.684169
		1.5				0.261353	−1.465483	0.738646
10	0.1	1	0.3			0.314332	−1.353698	0.685667
			0.6			0.289651	−1.300527	0.710348
			0.8			0.289522	−1.267200	0.710477
10	0.1	0.1	1	0.7		0.238458	−0.991674	0.533079
				1.2		0.348424	−0.986201	0.781890
				1.7		0.431920	−0.981895	0.965734
10	0.1	1	0.9	1	0.3	0.255546	−1.248268	0.744453
					0.5	0.254600	−1.241304	0.745398
					0.7	0.247357	−1.240469	0.752642

Furthermore, the behaviours on various values of parameters Pr, α, M, B, γ and λ on the velocity and temperature of fluid are depicted from Figs. 1 to 12. An increasing trend on velocity can be seen in the larger value of M and λ as captured in Figs. 5 and 11. This behaviour shows that the properties of those parameters characterises the ability to exchange thermal energy with its surroundings. Meanwhile, a contradicting behaviour can be seen for larger values of Pr, B, α and γ as illustrated in Figs. 1, 3, 7, and 9. The temperature distribution showed increasing trend for the parameters α, Pr and λ while the opposite trend was observed for γ, M and B. These trends happened due to the respective parameters with properties to absorb and release the energy to the fluid.

All the figures indicate, at far from the plate, that the velocity and temperature profiles of fluid asymptotically approached zero, which has fittingly fulfilled the boundary condition.

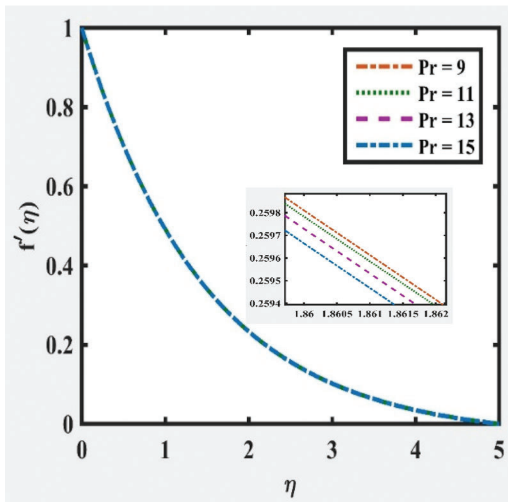

Figure 1: Variation of $f'(\eta)$ at $M = \gamma = 1$, $B = 0.1$, $\lambda = 3$ and $\alpha = 0.3$ for various values of Pr

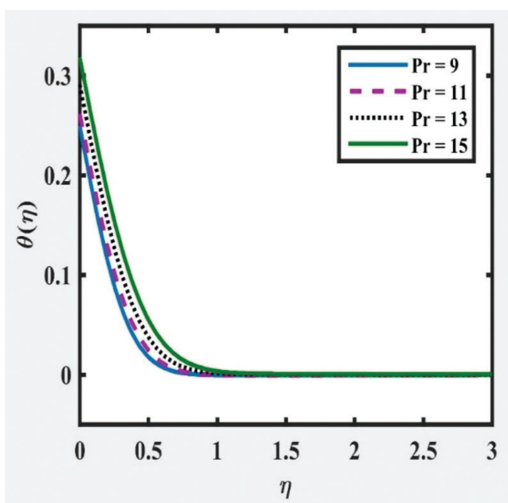

Figure 2: Variation of $\theta(\eta)$ at $M = \gamma = 1$, $B = 0.1$, $\lambda = 3$ and $\alpha = 0.3$ for various values of Pr

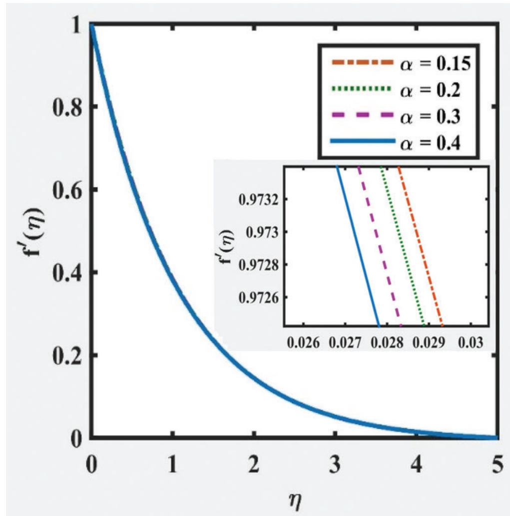

Figure 3: Variation of $f'(\eta)$ at $B = \lambda = 0.1$ and $\Pr = 10$ for various values of α

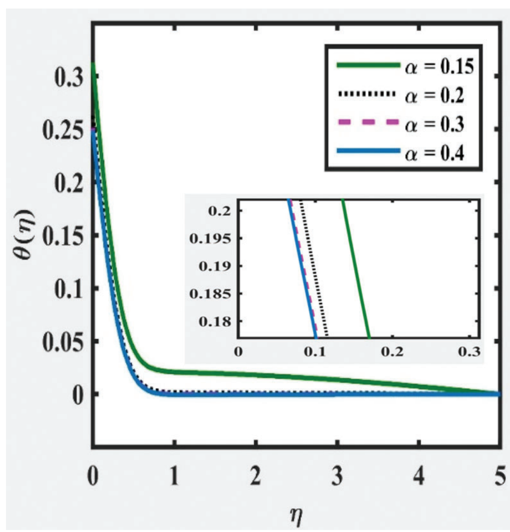

Figure 4: Variation of $\theta(\eta)$ at $M = \gamma = 1$, $B = \lambda = 0.1$ and $\Pr = 10$ for various values of α

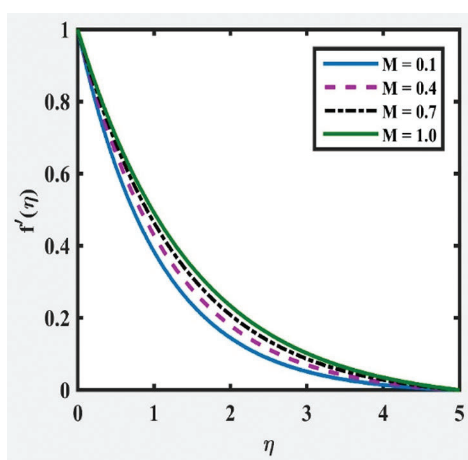

Figure 5: Variation of $f'(\eta)$ at $B = 0.5$, $\alpha = 0.1$, $\gamma = 1$, $\lambda = 0.01$ and $\Pr = 10$ for various values of M

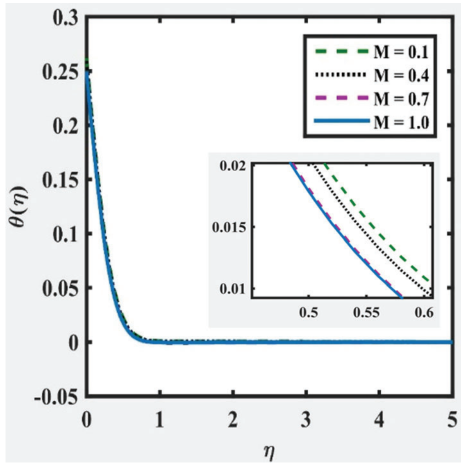

Figure 6: Variation of $\theta(\eta)$ at $B = 0.5$, $\alpha = 0.1$, $\gamma = 1$, $\lambda = 0.01$ and $\Pr = 10$ for various values of M

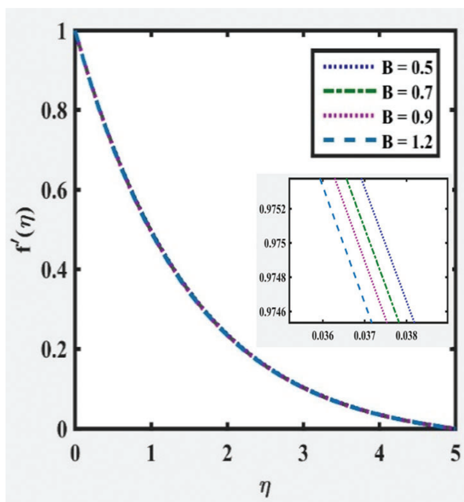

Figure 7: Variation of $f'(\eta)$ at $M = \gamma = 1$, $\alpha = \lambda = 0.1$ and $\Pr = 10$ for various values of B

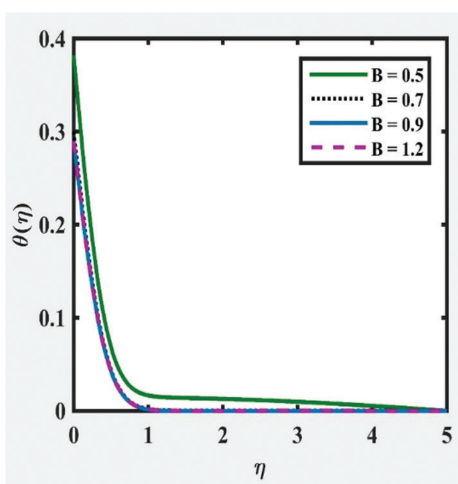

Figure 8: Variation of $\theta(\eta)$ at $M = \gamma = 1$, $\alpha = \lambda = 0.1$ and $\Pr = 10$ for various values of B

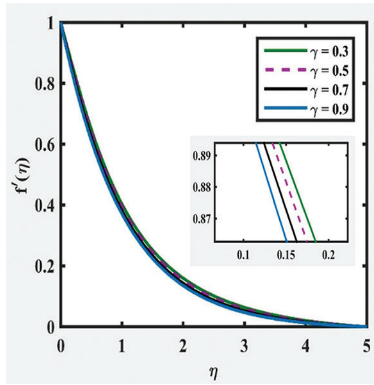

Figure 9: Variation of $f'(\eta)$ at $\lambda = 3$, $\Pr = 10$ and $M = B = \alpha = 0.1$ for various values of γ

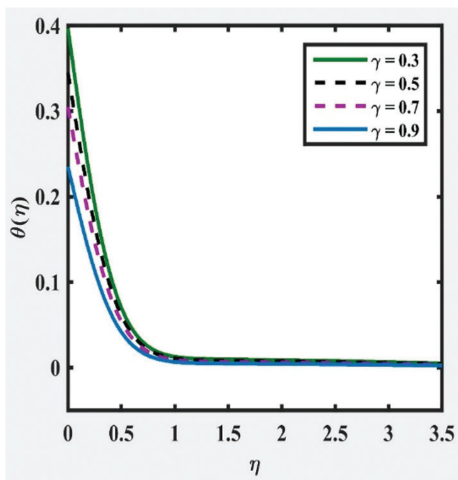

Figure 10: Variation of $\theta(\eta)$ at $\lambda = 3$, $\Pr = 10$ and $M = B = \alpha = 0.1$ for various values of γ

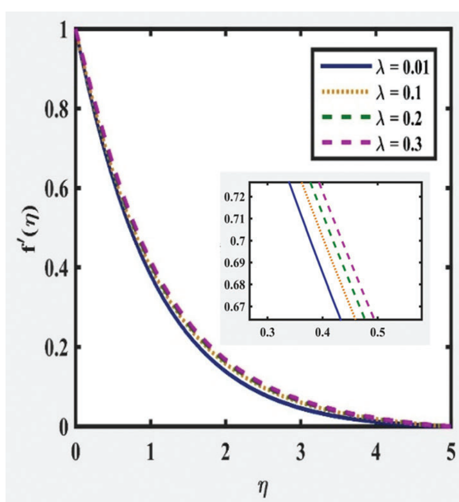

Figure 11: Variation of $f'(\eta)$ at $M = \gamma = 1$, $B = \alpha = 0.1$ and $\Pr = 10$ for various values of λ

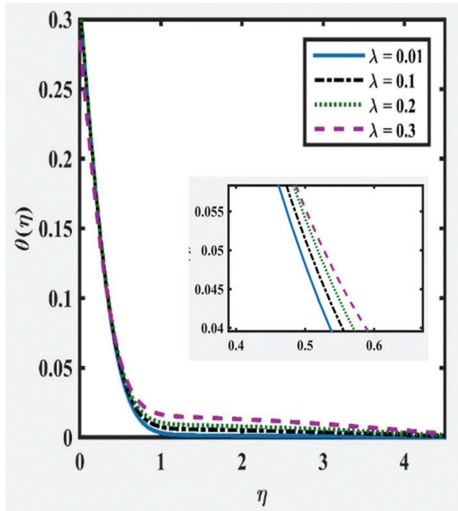

Figure 12: Variation of $\theta(\eta)$ at $M = \gamma = 1$, $B = \alpha = 0.1$ and Pr $= 10$ for various values of λ

6 Conclusion

This present research has integrated the mixed convective flow of an Eyring Powell fluid over a vertically stretched surface that was reviewed by highlighting the effects of temperature-dependent viscosity involving the parameters of Pr, α, M, B, γ and λ. From the mathematical analysis, a similar trend can be noticed in the motion and temperature distributions of fluid, respectively, when parameters were increased. The results of the parameters are illustrated in the specified graphs and tables. Nevertheless, the variations on the velocity distribution as well as fluid temperature portrayed the importance of the parameters investigated. The findings in this study contribute to a better understanding of the characteristics of fluid flow and its advancement.

Funding Statement: This project has been supported by Ministry of Higher Education and Universiti Malaysia Pahang through RDU182307.

Conflicts of Interest: The authors declare no conflicts of interest to report regarding the present study.

References

[1] B. Gireesha, G. Roopa and C. Bagewadi, "Effect of viscous dissipation and heat source on flow and heat transfer of dusty fluid over unsteady stretching sheet," *Applied Mathematics and Mechanics*, vol. 33, no. 8, pp. 1001–1014, 2012.

[2] T. Hayat, S. Shehzad, A. Alsaedi and M. Alhothuali, "Mixed convection stagnation point flow of Casson fluid with convective boundary conditions," *Chinese Physics Letters*, vol. 29, no. 11, pp. 114704, 2012.

[3] M. Turkyilmazoglu and I. Pop, "Heat and mass transfer of unsteady natural convection flow of some nanofluids past a vertical infinite flat plate with radiation effect," *International Journal of Heat and Mass Transfer*, vol. 59, pp. 167–171, 2013.

[4] E. Elbashbeshy, H. Asker, K. Abdelgaberc and E. Sayed, "Heat transfer over a stretching surface with variable thickness embedded in porous medium in the presence of maxwell fluid," *Journal of Applied Mechanical Engineering*, vol. 7, pp. 307, 2018.

[5] M. Yousfi, S. Alix, M. Lebeau, J. Soulestin, M. F. Lacrampe *et al.,* "Evaluation of rheological properties of non-Newtonian fluids in micro rheology compounder: Experimental procedures for a reliable polymer melt viscosity measurement," *Polymer Testing*, vol. 40, pp. 207–217, 2014.

[6] S. Kakac, Y. Yener and A. Pramuanjaroenkij, *Convective Heat Transfer*. Boca Raton, Florida, USA: CRC Press, 2013.

[7] T. Hayat, M. Waqas, S. Shehzad and A. Alsaedi, “Mixed convection radiative flow of Maxwell fluid near a stagnation point with convective condition,” *Journal of Mechanics*, vol. 29, no. 3, pp. 403–409, 2013.

[8] A. R. M. Kasim, N. F. Mohammad, S. Shafie and I. Pop, “Constant heat flux solution for mixed convection boundary layer viscoelastic fluid,” *Heat and Mass Transfer*, vol. 49, no. 2, pp. 163–171, 2013.

[9] N. S. Arifin, S. M. Zokri, A. R. M. Kasim, M. Z. Salleh, N. F. Mohammad *et al.,* “Aligned magnetic field of two-phase mixed convection flow in dusty Casson fluid over a stretching sheet with Newtonian heating,” *Journal of Physics: Conference Series*, vol. 890, no. 1, 012001, 2017.

[10] A. R. M. Kasim, N. S. Arifin, S. M. Zokri and M. Z. Salleh, “Flow and heat transfer of aligned magnetic field with Newtonian heating boundary condition,” *MATEC Web of Conferences*, vol. 189, 01005, 2018.

[11] M. Waqas, M. Farooq, M. I. Khan, A. Alsaedi, T. Hayat *et al.,* “Magnetohydrodynamic (MHD) mixed convection flow of micropolar liquid due to nonlinear stretched sheet with convective condition,” *International Journal of Heat and Mass Transfer*, vol. 102, pp. 766–772, 2016.

[12] R. Mahat, N. A. Rawi, A. R. M. Kasim and S. Shafie, “Mixed convection boundary layer flow of viscoelastic nanofluid past a horizontal circular cylinder: Case of constant heat flux,” *Journal of Physics: Conference Series*, vol. 890, no. 1, 012052, 2017.

[13] J. C. Umavathi, A. Chamkha and S. Mohiuddin, “Combined effect of variable viscosity and thermal conductivity on free convection flow of a viscous fluid in a vertical channel,” *International Journal of Numerical Methods for Heat & Fluid Flow*, vol. 51, pp. 71–86, 2016.

[14] M. A. El-Aziz, “Unsteady mixed convection heat transfer along a vertical stretching surface with variable viscosity and viscous dissipation,” *Journal of the Egyptian Mathematical Society*, vol. 22, no. 3, pp. 529–537, 2014.

[15] W. N. Z. Amin, M. Qasim and S. Shafie, “G-jitter induced mixed convection flow between two parallel plates with newtonian heating,” *Science Proceedings Series*, vol. 1, no. 2, pp. 107–110, 2019.

[16] M. Kumari and G. Nath, “Steady mixed convection flow of Maxwell fluid over an exponentially stretching vertical surface with magnetic field and viscous dissipation,” *Meccanica*, vol. 49, no. 5, pp. 1263–1274, 2014.

[17] J. O. Juárez, J. F. Hinojosa, J. P. Xamán and M. P. Tello, “Numerical study of natural convection in an open cavity considering temperature-dependent fluid properties,” *International Journal of Thermal Sciences*, vol. 50, no. 11, pp. 2184–2197, 2011.

[18] J. Umavathi and O. Ojjela, “Effect of variable viscosity on free convection in a vertical rectangular duct,” *International Journal of Heat and Mass Transfer*, vol. 84, pp. 1–15, 2015.

[19] P. A. Córdoba, N. Silin and E. A. Dari, “Natural convection in a cubical cavity filled with a fluid showing temperature-dependent viscosity,” *International Journal of Thermal Sciences*, vol. 98, pp. 255–265, 2015.

[20] S. Bair, C. Mary, N. Bouscharain and P. Vergne, “An improved Yasutomi correlation for viscosity at high pressure,” in *Proc. of the Institution of Mechanical Engineers, Part J: Journal of Engineering Tribology*, vol. 227, no. 9, pp. 1056–1060, 2013.

[21] Y. Khan, Q. Wu, N. Faraz and A. Yildirim, “The effects of variable viscosity and thermal conductivity on a thin film flow over a shrinking/stretching sheet,” *Computers & Mathematics with Applications*, vol. 61, no. 11, pp. 3391–3399, 2011.

[22] M. S. Astanina, M. A. Sheremet and J. C. Umavathi, “Transient natural convection with temperature-dependent viscosity in a square partially porous cavity having a heat-generating source,” *Numerical Heat Transfer, Part A: Applications*, vol. 73, no. 12, pp. 849–862, 2018.

[23] M. Alim, S. Alam and M. Miraj, “Effects of volumetric heat source and temperature dependent viscosity on natural convection flow along a wavy surface,” *Procedia Engineering*, vol. 90, pp. 383–388, 2014.

[24] N. S. Akbar, D. Tripathi, Z. H. Khan and O. A. Bég, “A numerical study of magnetohydrodynamic transport of nanofluids over a vertical stretching sheet with exponential temperature-dependent viscosity and buoyancy effects,” *Chemical Physics Letters*, vol. 661, pp. 20–30, 2016.

[25] N. Parveen and M. A. Alim, “Effect of temperature-dependent variable viscosity on magnetohydrodynamic natural convection flow along a vertical wavy surface,” *ISRN Mechanical Engineering*, vol. 2011, no. 1, pp. 1–10, 2011.

[26] R. Ellahi, "The effects of MHD and temperature dependent viscosity on the flow of non-Newtonian nanofluid in a pipe: Analytical solutions," *Applied Mathematical Modelling*, vol. 37, no. 3, pp. 1451–1467, 2013.
[27] R. Kairi, P. Murthy and C. Ng, "Effect of viscous dissipation on natural convection in a non-Darcy porous medium saturated with non-Newtonian fluid of variable viscosity," *Open Conservation Biology Journal*, vol. 3, no. 1, pp. 1–8, 2011.
[28] P. M. Thakur and G. Hazarika, "Effects of variable viscosity and thermal conductivity on the MHD flow of micropolar fluid past an accelerated infinite vertical insulated plate," *International Journal of Heat and Technology*, vol. 33, no. 3, pp. 73–78, 2015.
[29] B. K. Jha and B. Aina, "Investigation of temperature-dependent viscosity on steady, fully developed mixed convection flow in a vertical microchannel: An exact solution," *International Journal of Fluid Mechanics Research*, vol. 44, no. 4, pp. 357–373, 2017.
[30] N. S. Akbar, A. Ebaid and Z. Khan, "Numerical analysis of magnetic field effects on Eyring-Powell fluid flow towards a stretching sheet," *Journal of Magnetism and Magnetic Materials*, vol. 382, pp. 355–358, 2015.
[31] A. Ara, N. A. Khan, H. Khan and F. Sultan, "Radiation effect on boundary layer flow of an Eyring-Powell fluid over an exponentially shrinking sheet," *Ain Shams Engineering Journal*, vol. 5, no. 4, pp. 1337–1342, 2014.
[32] M. Malik, A. Hussain and S. Nadeem, "Boundary layer flow of an Eyring-Powell model fluid due to a stretching cylinder with variable viscosity," *Scientia Iranica*, vol. 20, no. 2, pp. 313–321, 2013.
[33] S. Nadeem and S. Saleem, "Mixed convection flow of Eyring-Powell fluid along a rotating cone," *Results in Physics*, vol. 4, pp. 54–62, 2014.
[34] T. Hayat, S. Ali, M. A. Farooq and A. Alsaedi, "On comparison of series and numerical solutions for flow of Eyring-Powell fluid with Newtonian heating and internal heat generation/absorption," *PLoS One*, vol. 10, no. 9, 2015.
[35] M. Malik, T. Salahuddin, A. Hussain and S. Bilal, "MHD flow of tangent hyperbolic fluid over a stretching cylinder: Using Keller box method," *Journal of Magnetism and Magnetic Materials*, vol. 395, pp. 271–276, 2015.
[36] M. Malik, I. Khan, A. Hussain and T. Salahuddin, "Mixed convection flow of MHD Eyring-Powell nanofluid over a stretching sheet: A numerical study," *AIP Advances*, vol. 5, no. 11, 117118, 2015.
[37] I. Khan, M. Malik, T. Salahuddin, M. Khan and K. U. Rehman, "Homogenous-heterogeneous reactions in MHD flow of Powell-Eyring fluid over a stretching sheet with Newtonian heating," *Neural Computing and Applications*, vol. 30, no. 11, pp. 3581–3588, 2018.
[38] A. Zeeshan, S. Abbasbandy and S. Rashidi, "Joules and Newtonian heating effects on stagnation point flow over a stretching surface by means of genetic algorithm and Nelder-Mead method," *International Journal of Numerical Methods for Heat & Fluid Flow*, vol. 25, no. 3, pp. 665–684, 2015.
[39] T. Salahuddin, M. Malik, A. Hussain, S. Bilal and M. Awais, "Effects of transverse magnetic field with variable thermal conductivity on tangent hyperbolic fluid with exponentially varying viscosity," *AIP Advances*, vol. 5, no. 12, pp. 127103, 2015.
[40] T. Javed, N. Ali, Z. Abbas and M. Sajid, "Flow of an Eyring-Powell non-Newtonian fluid over a stretching sheet," *Chemical Engineering Communications*, vol. 200, no. 3, pp. 327–336, 2013.
[41] A. Bejan, *Convection Heat Transfer*. 4^{th} ed., New York: Springer, 2013.
[42] W. M. Kays, *Convective Heat and Mass Transfer*. New York, Tata McGraw-Hill Education, 2012.
[43] H. A. M. Al-Sharifi, A. R. M. Kasim and M. Z. Salleh, "Effect of newtonian heating on the mixed convection boundary layer flow of Eyring-Powell fluid across a nonlinearly stretching sheet," *Journal of Engineering and Applied Sciences*, vol. 11, no. 11, pp. 2372–2377, 2016.
[44] M. Z. Salleh, R. Nazar and I. Pop, "Boundary layer flow and heat transfer over a stretching sheet with Newtonian heating," *Journal of the Taiwan Institute of Chemical Engineers*, vol. 41, no. 6, pp. 651–655, 2010.
[45] M. Qasim, I. Khan and S. Shafie, "Heat transfer in a micropolar fluid over a stretching sheet with Newtonian heating," *PLoS One*, vol. 8, no. 4, 2013.